Heisenberg's uncertainty principle and the diffraction of light

Andrew Hanzhuo Zhang

Abstract

To test the hypothesis that the diffraction of light is a macroscopic manifestation of photons obeying Heisenberg's uncertainty principle, I designed an experiment to investigate whether the inverse correlation between the uncertainties of position and momentum of elementary particles asserted by Heisenberg's uncertainty principle can be derived from the relationship between the dispersion of photons diffracting through a single narrow slit and the slit's width. After analyzing the results of my experiment with respect to Heisenberg's uncertainty principle, I was able to establish the value of Planck's constant as $h \approx (7\pm3)\times10^{-34}$ J s, which only deviates from its original value of $h \approx 6.63\times10^{-34}$ J s by 4.2%. This confirmed my hypothesis within the acceptable margin of error of my experiment, and thus proved Heisenberg's uncertainty principle to be a more complete explanation for why the diffraction of light occurs than Huygen's principle as used by most physics textbooks. This research paper achieved grade A for being awarded 31/34 marks by the International Baccalaureate Organization.

Table of Contents

1. Introduction

1.1 Background

Most textbooks explain why diffraction occurs when waves encounter an obstacle with Huygen's principle, which states that "each point on a wavefront acts as a point source that emits spherical wavelets, and at any later time, the total wavefront is the envelope that encloses all of these wavelets" *(University of Colorado Boulder)*. However, with reference to *Figure-1* and *Figure-2* *(Georgia State University, Single Slit Diffraction)*, Huygen's principle of wavefront does not explain why the diffraction pattern of a coherent monochromatic light source passing through a single slit becomes more dispersed as the slit narrows.

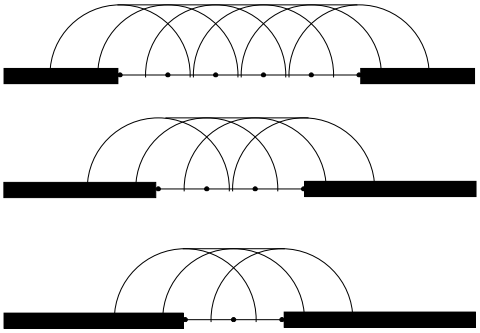

Figure-1: Diffraction according to Huygen's principle of wavefronts, diffraction patterns should become more dispersed when the slit is wider.

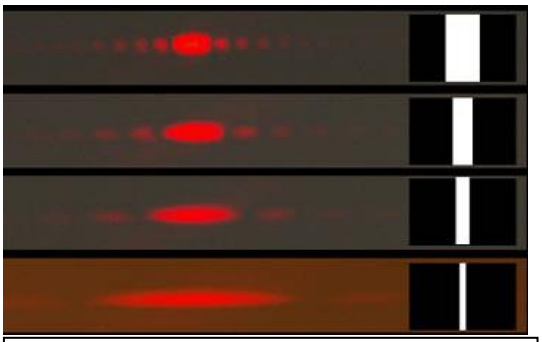

Figure-2: Diffraction observed in real life, diffraction pattern becomes less dispersed when the slit is wider. *(Georgia State University, Single Slit Diffraction)*

After reading about Heisenberg's uncertainty principle in *Topic-12* of the HL physics syllabus, I realized that it potentially offers an exquisite explanation towards why the diffraction of light occurs that accounts for aforementioned phenomenon. This lead to the research question: "***Does the relationship between the width of a single slit and the dispersion of the diffraction pattern formed when monochromatic coherent light passes through it demonstrate Heisenberg's uncertainty principle?***"

1.2 Theory

The uncertainty principle asserts that "there is a fundamental limit to the precision with which certain pairs of physical properties of a particle, such as position and momentum, can be known simultaneously, which the more precisely the position of some particle is determined, the less precisely its momentum can be known and vice versa" *(University of Sydney)*. Heisenberg's uncertainty principle for position and momentum is mathematically expressed as:

$$\Delta x \, \Delta p \geq \frac{h}{4\pi} \quad [1]$$

, where h is Planck's constant and the variables Δx and Δp stands for the uncertainties of a simultaneous measurement of position x and momentum p of a quantum object.

Heisenberg's uncertainty principle becomes relevant to the diffraction of light when we take the particle-wave duality of light into account, which allows light as particles to theoretically possess positions and momenta. The simultaneous uncertainty of position and momentum for photons passing through a narrow slit can be derived by considering *Figure-3*, where the y-axis measures the linear position of a photon perpendicular to the slit, and p_y is the photon's component momentum along the y-axis. The range of possible y positions of photons passing through the

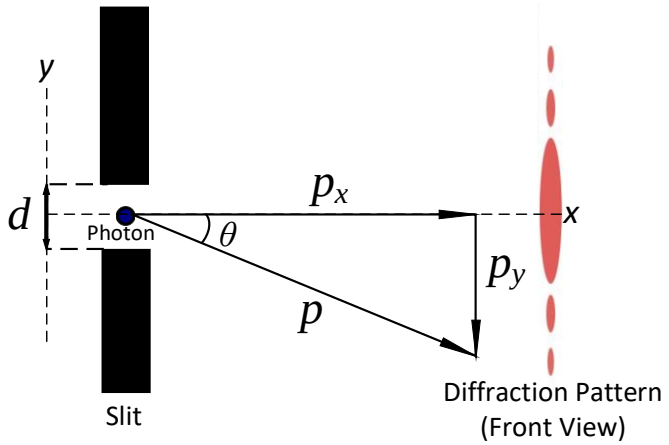

Figure-3: Geometry of single slit diffraction in relation to a photon's momentum.

slit is restricted within the width of the slit d, hence a narrower slit would mean that we are less uncertain about the linear position y of any individual photon passing through the slit. Simultaneously, the same photons will exit the slit at different angles of θ due to the range of different component momenta p_y they possess. Given that the relationship between θ and p_y is positive within the domain of $-\frac{\pi}{2} \leq \theta \leq \frac{\pi}{2}$, a diffraction pattern that is more dispersed along the y-axis would mean that we are more uncertain about the component momentum p_y of each individual diffracting photon.

2. Hypothesis

2.1 Hypothesis based on theory

My hypothesis is that the phenomena of diffraction patterns becoming more dispersed as the slit narrows is a direct result of photons obeying Heisenberg's uncertainty principle. With respect to the stated theory, the following line of reasoning shows how Heisenberg's uncertainty principle can cause light to diffract after entering a narrow slit and demonstrate this phenomena:

When a photon enters a slit that is narrow enough to reduce Δy to the point that the product of Δp_y and Δy drops to fundamental limit asserted by Heisenberg's uncertainty principle, Δp_y of the photon will be forced to increase to accommodate Heisenberg's inequality [1][1]. Given that light will always travel at the same speed in the same medium, this increase in Δp_y can only result the photon having a higher probability of directionally deviating from its previous trajectory, causing it to have a higher probability of exiting the slit at a different angle from the angle that it entered. An observable stream of light would contain a great number of photons, hence every photon's increased tendency to deviate from the angle that it enters the slit from will statistically manifest as the stream of light dispersing after exiting the slit, which causes the phenomenon that we call diffraction. Hence, passing light through narrower slits will cause a greater increase of Δp_y, which in turn causes a greater probability for individual photons to deviate from its previous trajectory at a greater angle and resulting in a more dispersed diffraction pattern to be observed at a constant distance.

---

[1] [1]: $\Delta x \, \Delta p \geq \frac{h}{4\pi}$ page 5

2.2 Mathematical interpretation of hypothesis

First, it should be noted that the original inequality [1] describes the behavior of the uncertainties of position and momentum in three-dimensional space, but the variables Δy and Δp_y defined in the introduction are one-dimensional, as they are only measured along the *y*-axis on *Figure-3*. Hence the fundamental limit of the product of Δy and Δp_y should be some unknown constant other than $\frac{h}{4\pi}$ stated in [1].

Furthermore, it should be realized that the tradeoff between the uncertainties of momentum and position due to Heisenberg's uncertainty principle will only occur when the product of the pair of uncertainties exceed their fundamental lower-bounds asserted by the inequality. Hence the product of Δy and Δp_y has to be exactly equal to the fundamental limit for diffraction to happen as hypothesized.

Based on the two aforementioned points, the anticipated relationship between Δy and Δp_y for diffracting photons is:

$$\Delta y \, \Delta p_y = k \quad [2]$$

$$k \in \mathbb{R}^+$$

, where *k* is the unknown constant representing the fundamental limit of the product of the one-dimensional uncertainty of the diffracting photons' position and momentum.

Subsequently, the hypothesis can be verified by investigating whether $\Delta p_y \propto \frac{1}{\Delta y}$ holds true for diffracting photons through experiment.

2.3 Literature

Werner Heisenberg himself proposed in his 1930 publication '*Principles of Quantum Theory'* that for electrons passing through a narrow slit, the product of one-dimensional uncertainties of position *x* and momentum p_x satisfies the inequality:

$$\Delta x \, \Delta p_x \gtrapprox h \quad [3]$$

(Heisenberg et al. 14)

$$h \approx 6.63 \times 10^{-34} \text{ J s}$$

Richard Feynman later explained in one of his lectures that this inequality is obtained by assuming that most diffracting electrons will fall within the central maxima of the diffraction pattern formed *(Belle)*, and Louis de Broglie's hypothesis that

$$\lambda = \frac{h}{p} \quad [4] \qquad \textit{(Belle)}$$

holds true for electrons, where *p* is the momentum of the electron, λ is the wavelength of the electron, and *h* is Planck's constant.

Although photons and electrons are different particles, they both possess particle-wave duality and therefore will diffract following the same principles when passed through a narrow slit, which means that they should share the same uncertainty relation during diffraction. Hence if we can prove for the anticipated relation that:

$$\Delta y \, \Delta p_y \cong h \quad [5]$$

through experiment, it would further evidence that the diffraction of light does exhibit Heisenberg's uncertainty principle.

3. Experiment Design

3.1 Variables

An experiment is designed to study how the dispersion of diffraction patterns from a monochromatic coherent light source vary when the slit width d changes. The width of the central maximum w and the maximum intensity I_0 of each distinct diffraction pattern is measured to evaluate its magnitude of dispersion.

The ultimate objective of this experiment is to determine whether the relationship between Δy and Δp_y of diffracting photons conforms with the hypothesis. Δy of the diffracting photons is derived from the proximate independent variable d changed in this experiment, while Δp_y of the diffracting photons is derived by studying the dispersion of diffraction patterns formed at different slit widths through the proximate dependent variables w and I_0 measured in this experiment.

The controlled variables for this experiment are tabulated on *Table-1*.

Table-1: Variables controlled during experimental measurements of I_0 and w

Symbol	Definition	Control value	Reason for control
D	**Perpendicular Distance** between the slit and the wall where the diffraction pattern is projected.	1±0.005 m	The diffraction pattern changes independently of d when D changes. (see [8][2])
λ	**Wavelength** of the light source used.	632.8 nm (Helium-neon laser)	The diffraction pattern changes independently of d when λ changes. (see [8])
θ_i	**Incident angle** of light source on the slit.	90°±0.5°	The diffraction pattern would be distorted if $\theta_i \neq 90°$.
P	**Output power** of the laser source.	1 mW	I_0 is dependent on P.
L_a	**Ambient** luminosity.	≤2±1 Lux	Ambient light interferes with I_0 measurement.

[2] [8]: $w = \frac{2D\lambda}{d}$ page 15

3.2 Experiment setup

3.2.1 Description of setup

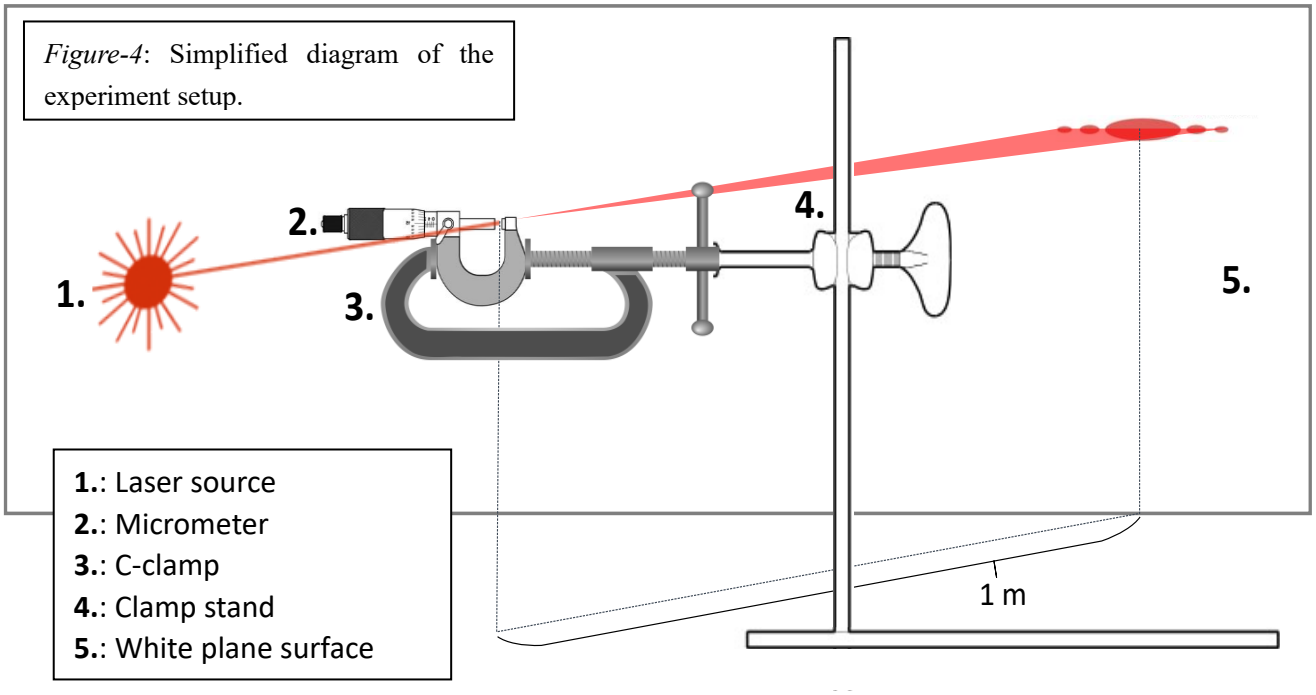

Figure-4: Simplified diagram of the experiment setup.

As seen on *Figure-4*, the slit width d is controlled by a Vernier micrometer, with 1×10^{-5} m being the smallest controllable unit. The micrometer is suspended at an appropriate height by a C-clamp attached to a clamp stand, and a spirit level is used in the process of positioning the micrometer to ensure that the slit is perpendicular to the ground. The laser source used is a Griffin class-II helium-neon laser box that has a constant output power of 1mW to control the variable P.

In addition to *Figure-4*, a straight pencil line is drawn right beneath and parallel to the slit of the micrometer that extends back to meet a protractor that is attached to the laser source to control the variable θ_i at 90°±0.5°. This measure is taken to ensure minimum distortion of the diffraction pattern produced. A meter ruler is also placed perpendicularly beneath the micrometer and extends to the white plane surface to

control the variable D at 1 ± 0.005 m. To hold the apparatus more firmly in place, blu tack is applied between the C-clamp and the micrometer to prevent slipping; Pieces blu tack is also placed at the bottom of the clamp stand to secure the setup in place.

3.2.2 Capacity of setup

A test-run is conducted to determine the domain of slit widths that can be tested on this setup.

While the light source ceases to diffract at $d = 3.70\times10^{-4} \pm 5\times10^{-6}$ m, the projected diffraction pattern becomes unmeasurable at $d = 5.0\times10^{-5} \pm 5\times10^{-6}$ m. Hence the testable domain of slit width d on this setup is $\{3.70\times10^{-4}\text{ m} \geq d \geq 5.0\times10^{-5}\text{ m}\}$.

3.3 Measurement

3.3.1 Measuring w

The width of the central maximum of each diffraction pattern is measured using a metal Vernier caliper that has a smallest unit of measurement of 0.0001m. To measure the width of the central maximum, the Vernier caliper is position flat against the plane surface above the diffraction pattern, and adjusted until the lower jaws aligns with the boundary between the central maximum and the first minima as seen on *Figure-5*.

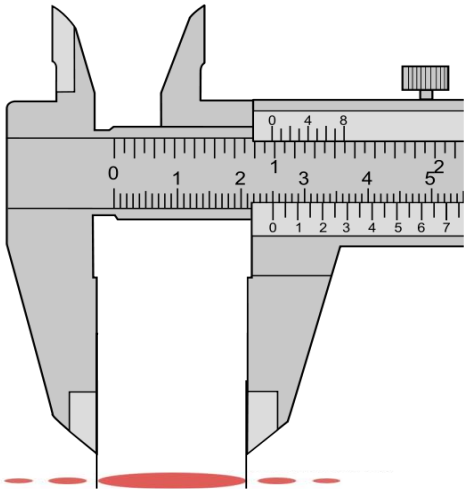

Figure-5: Measuring the width of a diffraction pattern with a Vernier caliper

It must be noted that the transition from bright to dark fringes on a diffraction pattern is continuous, which makes the measurement of *w* subjective to some extent. To compensate for this effect, four trials of *w* measurements are taken for each distinct diffraction pattern, and the final results are compared with theoretical values to validate accuracy.

3.3.2 Measuring I_0

The maximum intensity on each diffraction pattern is measured by using a digital Lux-meter that is composed of a light sensor connected to a LabQuest 2 computer interface. The smallest unit of measurement on this piece of apparatus is 1 Lux. To measure the maximum intensity, the sensor is slowly shifted across the diffraction pattern, while the intensity received by the sensor at each position is logged on a

spreadsheet at the rate of 3 readings per second. The maximum value is then taken from the spreadsheet as the I_0 for the trial. Four trials of I_0 measurements are taken for each diffraction pattern to improve accuracy. To control the variable L_a, each trial of measurement for I_0 is always preceded by a measurement of the ambient luminosity by the same equipment to ensure $L_a \leq 2 \pm 1$ Lux.

3.3.3 Treatment of errors and uncertainties

To simultaneously account for the range of uncertainty in repeated trials of raw measurements and the instrumental error of the measuring apparatus in individual measurements, an aggregate error is calculated for every measured trial average as follows:

$$\text{Aggregate error} = \frac{\text{Trial maximum} - \text{Trial minimum}}{2} + \sum \text{Instrument error}$$

In terms of propagating errors down into derived variables that are calculated from known values, we take the sum of all the relative errors associated with each value involved in the variable's calculation and multiply it by the calculated value of the variable, which that:

$$\text{Propagated error} = \sum \frac{\text{Associated error}}{\text{Value used in calculation}} \times \text{Calculated value}$$

For all tabulated results, uncertainty values are rounded to their first significant digit, while the values that they attach to are rounded to the same significant digit. Calculated theoretical values without uncertainties are to have the same number of significant digits as their corresponding raw measurements.

4. Data Processing

4.1 Proximate Result

4.1.1 Relationship between *d* and *w*

4.1.1.1 Theoretical value of *w*

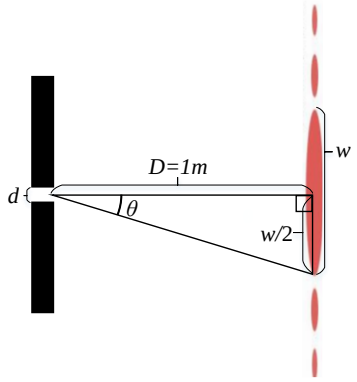

Figure-6: Geometry of single-slit diffraction patterns

The angle θ where the first minima occurs is calculated by the formula:

$$\theta = \frac{\lambda}{d} \quad [6]$$

, where λ is the wavelength of the light source, and d is the slit width. By applying [6] to *Figure-6*, it can be deduced that *w* is theoretically calculated by the equation:

$$w = 2 \times D \times \tan\frac{\lambda}{d} \quad [7]$$

Given that the small angle approximation $\sin\theta \approx \tan\theta \approx \theta$ applies to the scenario on *Figure-6*, where $D \gg d$, [7] can be simplified as:

$$w = \frac{2\,D\,\lambda}{d} \quad [8]$$

Substituting in D = 1 m and $\lambda = 6.238 \times 10^{-7}$ m into [8], we finally get:

$$w = \frac{12.656 \times 10^{-7}}{d} \quad [9]$$

All theoretical values of *w* tabulated on *Table-2* are calculated by [9].

4.1.1.2 Experiment data

Table-2: Relationship between width of slit *d* and width of principle maximum *w* on the diffraction pattern

d: Width of slit (m) *± 0.000005 m instrument error*	*w*: Measured width of diffraction pattern principle maximum (m)					
	Trial 1	Trial 2	Trial 3	Trial 4	Trial average *with aggregate error*	Calculated Theoretical Value
	± 0.00005 m instrument error					
0.000370	0.00340	0.00340	0.00330	0.00340	0.0034 ± 0.0001	0.00342
0.000360	0.00340	0.00350	0.00340	0.00340	0.0034 ± 0.0001	0.00352
0.000350	0.00340	0.00340	0.00350	0.00340	0.0034 ± 0.0001	0.00362
0.000340	0.00340	0.00340	0.00350	0.00350	0.0035 ± 0.0001	0.00372
0.000330	0.00340	0.00340	0.00350	0.00350	0.0035 ± 0.0001	0.00384
0.000320	0.00350	0.00350	0.00360	0.00350	0.0035 ± 0.0001	0.00396
0.000310	0.00350	0.00350	0.00360	0.00360	0.0036 ± 0.0001	0.00408
0.000300	0.00350	0.00340	0.00370	0.00380	0.0036 ± 0.0003	0.00422
0.000290	0.00400	0.00360	0.00380	0.00400	0.0039 ± 0.0003	0.00436
0.000280	0.00440	0.00420	0.00410	0.00430	0.0043 ± 0.0002	0.00452
0.000270	0.00440	0.00430	0.00420	0.00440	0.0043 ± 0.0002	0.00469
0.000260	0.00450	0.00420	0.00430	0.00440	0.0044 ± 0.0002	0.00487
0.000250	0.00460	0.00460	0.00450	0.00460	0.0046 ± 0.0001	0.00506
0.000240	0.00450	0.00490	0.00490	0.00460	0.0047 ± 0.0003	0.00527
0.000230	0.00510	0.00540	0.00510	0.00490	0.0051 ± 0.0003	0.00550
0.000220	0.00500	0.00570	0.00530	0.00520	0.0053 ± 0.0004	0.00575
0.000210	0.00520	0.00610	0.00530	0.00540	0.0055 ± 0.0005	0.00603
0.000200	0.00540	0.00620	0.00560	0.00570	0.0057 ± 0.0005	0.00633
0.000190	0.00580	0.00660	0.00580	0.00630	0.0061 ± 0.0005	0.00666
0.000180	0.00600	0.00720	0.00620	0.00680	0.0066 ± 0.0007	0.00703
0.000170	0.00640	0.00790	0.00650	0.00730	0.0070 ± 0.0008	0.00744
0.000160	0.00640	0.00810	0.00710	0.00770	0.0073 ± 0.0009	0.00791
0.000150	0.00710	0.00890	0.00740	0.00790	0.008 ± 0.001	0.00844
0.000140	0.00830	0.00920	0.00920	0.00820	0.0087 ± 0.0006	0.00904
0.000130	0.00800	0.00950	0.00960	0.00870	0.0090 ± 0.0009	0.00974
0.000120	0.00850	0.01010	0.01170	0.00920	0.010 ± 0.002	0.01055
0.000110	0.00920	0.01330	0.01290	0.01230	0.012 ± 0.002	0.01151
0.000100	0.01000	0.01120	0.01310	0.01290	0.012 ± 0.002	0.01266
0.000090	0.01170	0.01570	0.01560	0.01390	0.014 ± 0.002	0.01406
0.000080	0.01340	0.02370	0.01630	0.01430	0.017 ± 0.005	0.01582
0.000070	0.01590	0.01900	0.02110	0.01870	0.019 ± 0.003	0.01808
0.000060	0.02380	0.02290	0.02320	0.02140	0.023 ± 0.001	0.02109
0.000050	0.02580	0.03430	0.02730	0.02430	0.028 ± 0.005	0.02531

Figure-7: Relationship between width of slit *d* and width of principle maxima *w* on the diffraction pattern

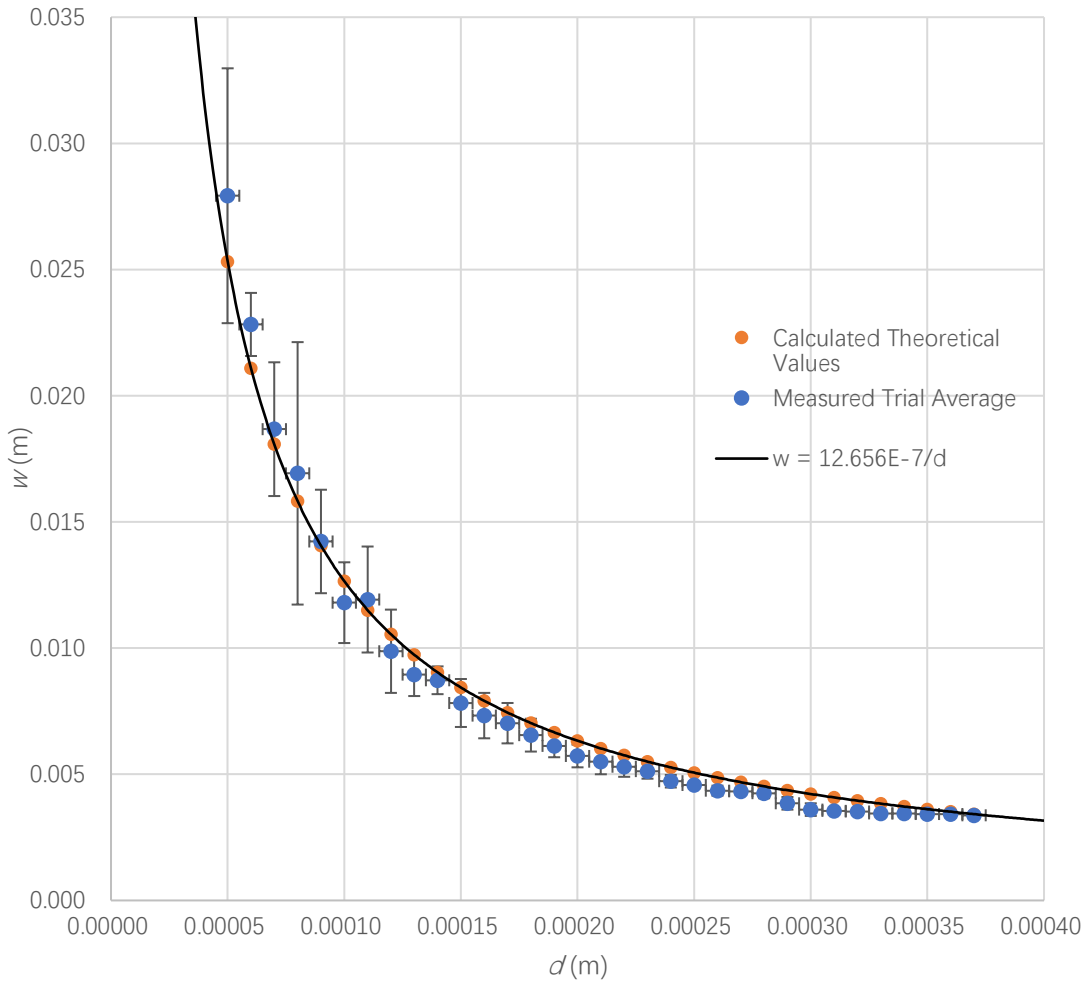

Figure-7 shows that the measured values of *w* closely resemble the theoretical values calculated by [7], which largely lie within the acceptable range of errors and hence suggest that the measured values are valid and accurate. Since the first maxima will always pinpoint where the path difference of the diffracting light is $\frac{1}{2}\lambda$, the negative relationship between *d* and *w* supports that the diffraction pattern becomes more dispersed in the *y* direction as the slit narrows.

4.1.2 Relationship between I_0 and w

4.1.2.1 Converting luminous intensity into light intensity

The lux-meter used in the experiment measures luminous intensity in Lux instead of light intensity in W m^{-2}, hence luminous intensity must be converted into light intensity before proceeding with analysis. The conversion factor between Lux and W m^{-2}, lm W^{-1}, varies across the E-M spectrum, as light with different wavelength will have different brightness when emitted at the same frequency.

Although secondary research yielded no literature for the specific conversion factor at $\lambda = 632.8\,\text{nm}$, a table of conversion factors at other wavelengths (*Georgia state university)* was found and attached to the appendix. The contents of the table is graphically plotted on *Figure-8*.

Figure-8: Conversion factor between luminous intensity and light intensity at different wavelengths of E-M waves

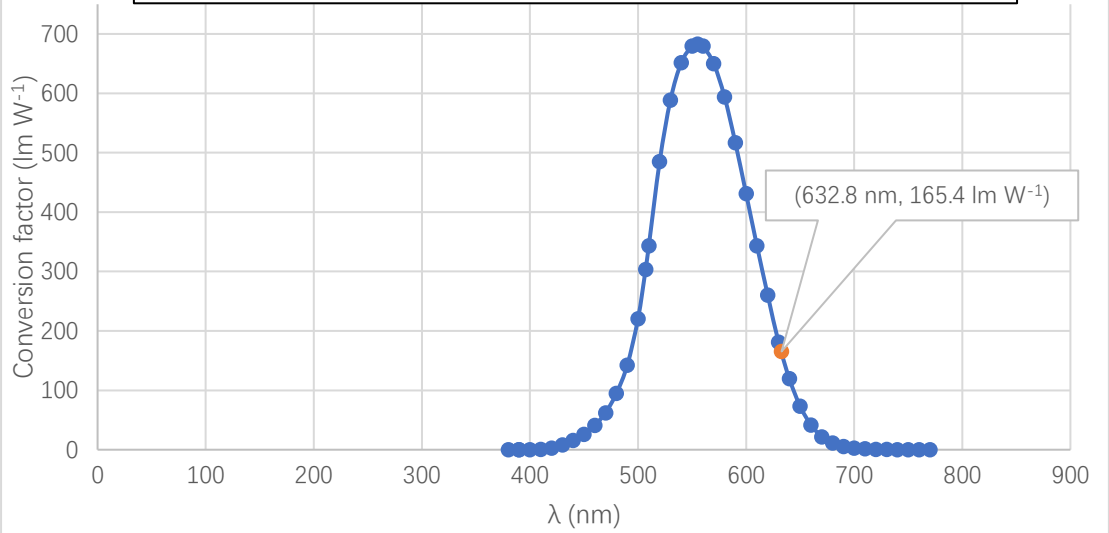

It can be deduced from *Figure-8* that the conversion factor between luminous intensity and light intensity is $\approx$165.4 lm W^{-1} at $\lambda = 632.8\,\text{nm}$, hence we can say for the helium-neon laser used in the experiment that:

$$1\ \text{Lux} = 165.4\ \text{W m}^{-2}\ \ [10]$$

4.1.2.2 Experiment data

Table-3: Relationship between width of slit *d* and maximum intensity I_0 on the diffraction pattern

d: Width of slit (m)	L_0: Measured maximum luminous intensity (Lux)					I_0: Calculated maximum intensity ($W\ m^{-2}$)
± 0.000005 m	Trial 1	Trial 2	Trial 3	Trial 4	Trial Average	
Instrument error	*± 1 Lux instrument error*				*with aggregate error*	*with propagated error*
0.000370	8417	8460	8459	8432	8440 ± 20	51.0 ± 0.1
0.000360	8106	8222	8214	8245	8200 ± 70	49.6 ± 0.4
0.000350	7689	8119	7807	8007	8000 ± 200	48 ± 1
0.000340	7913	7934	7601	7932	7800 ± 200	47 ± 1
0.000330	7468	7567	7321	7568	7500 ± 100	45.2 ± 0.8
0.000320	7276	7432	7213	7211	7300 ± 100	44.0 ± 0.7
0.000310	6904	7024	6876	7094	7000 ± 100	42.2 ± 0.7
0.000300	6583	6678	6489	6632	6600 ± 100	39.9 ± 0.6
0.000290	6397	6432	6452	6546	6460 ± 80	39.0 ± 0.5
0.000280	6301	6331	6405	6387	6360 ± 50	38.4 ± 0.3
0.000270	5400	6027	6014	6034	5900 ± 300	35.5 ± 1.9
0.000260	5661	5788	5491	5512	5600 ± 200	33.9 ± 0.9
0.000250	5150	4952	4932	5209	5100 ± 100	30.6 ± 0.8
0.000240	4789	4885	4723	4976	4800 ± 100	29.3 ± 0.8
0.000230	4568	4671	4610	4764	4700 ± 100	28.1 ± 0.6
0.000220	4322	4321	4524	4298	4400 ± 100	26.4 ± 0.7
0.000210	3872	3726	3955	3867	3900 ± 100	23.3 ± 0.7
0.000200	3399	3628	3824	4043	3700 ± 300	23 ± 2
0.000190	3317	3440	3547	3671	3500 ± 200	21 ± 1
0.000180	3427	3013	3282	3222	3236 ± 208	20 ± 1
0.000170	3108	3000	3112	3007	3060 ± 60	18.5 ± 0.3
0.000160	2867	2816	2996	2706	2800 ± 100	17 ± 1
0.000150	2230	2533	2432	2671	2500 ± 200	15 ± 1
0.000140	2006	1991	1783	2028	2000 ± 100	12 ± 1
0.000130	1438	1756	1801	1875	1700 ± 200	10 ± 1
0.000120	1447	1658	1672	1704	1600 ± 100	9.8 ± 0.8
0.000110	1166	1232	1532	1324	1300 ± 200	8 ± 1
0.000100	807	1027	904	1098	1000 ± 100	5.8 ± 0.9
0.000090	567	623	589	576	590 ± 30	3.6 ± 0.2
0.000080	434	498	395	414	440 ± 50	2.6 ± 0.3
0.000070	288	256	291	264	280 ± 20	1.7 ± 0.1
0.000060	165	185	178	187	180 ± 10	1.1 ± 0.1
0.000050	50	52	54	53	52 ± 3	0.32 ± 0.02

Figure-9: Relationship between width of slit *d* and maximum intensity I_0 of diffraction pattern

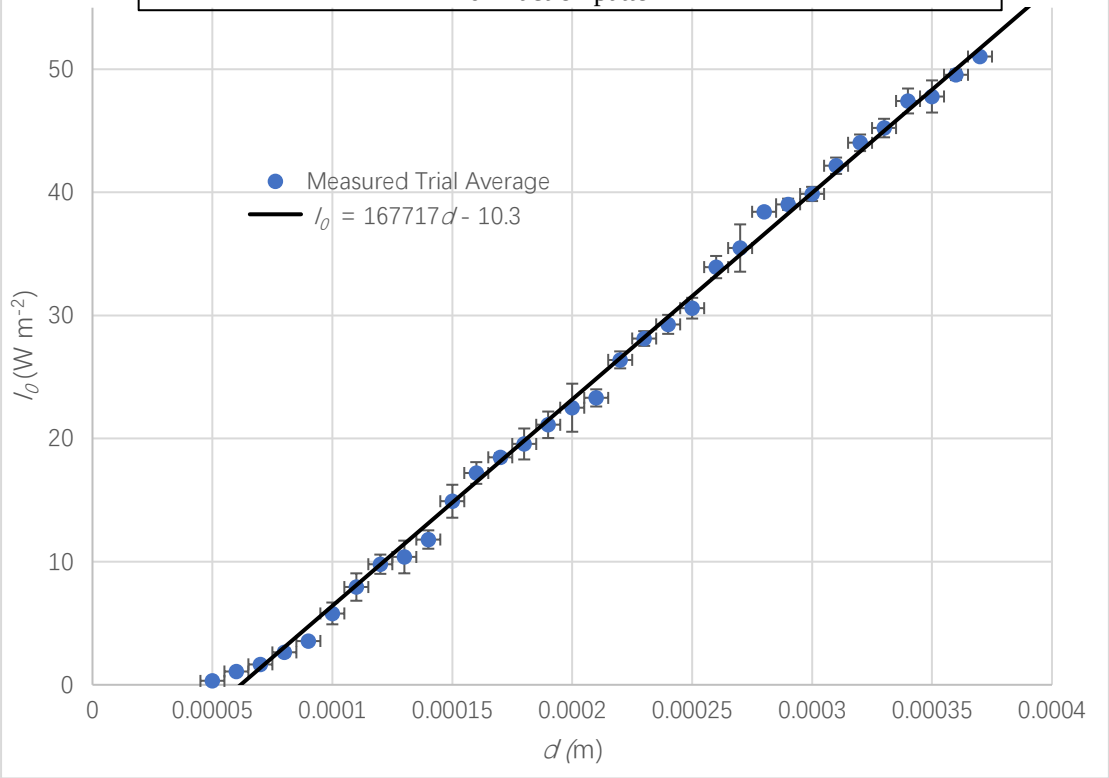

Since the output power *P* of the helium-neon laser is rated at 1 mW constant, the output intensity of the light source is constant. In the context that the collimated beams produced by lasers have minimum dispersion, the positive relationship between I_0 and *d* seen from *Figure-9* also supports that the diffraction pattern becomes more dispersed as the slit narrows.

Fitting a linear trend line through the data set seems to show that there is a systematic error, as it does not pass through the origin where it theoretically should, as there will be no light passing through when the slit width is zero. However, I_0 at narrower slit widths deviates from the linear trend, where the rate of change gradually decreases and the data tends toward the origin. While there is no literature to refer to, it can't be determined at this stage whether there is a systematic error or not, a possible reason for this observation is proposed under *Section-6.1* under evaluation.

4.2 Deriving ultimate variables

The uncertainty relation [1][3] between position *x* and momentum *p* is more formally known as:

$$\sigma_x \, \sigma_p \geq \frac{h}{4\pi} \quad [11] \qquad \textit{(University of New Mexico)}$$

, where the uncertainties Δx and Δp are defined by the standard deviations of position and momentum σ_x and σ_p. This shows that we can also derive Δy and Δp_y as the standard deviations of *y* and p_y if we can recreate the distribution of photons diffracting through the slit as functions of *y* and p_y from the proximate experiment results.

4.2.1 Quantifying photons

Quantifying photons is necessary for recreating the distribution of photons as a function of any variable. Since photons as quantum objects carry discrete quantities of energy, the most intuitive approach to quantify them is through energy.

The energy *E* of a single photon is calculated by the formula:

$$E = \frac{h\,c}{\lambda} \quad [12]$$

, where *c* is the speed of light, *h* is Planck's constant and λ is the wavelength of the photon. Given the light source used in this experiment is monochromatic, which means that each photon emitted will always carry the same quantity of energy according to [12], it can be deduced that:

$$\text{Photon flux} \propto \text{Light intensity} \quad [13]$$

[3] [1]: $\Delta x \, \Delta p \geq \frac{h}{4\pi}$ page 5

; Hence light intensity can be used as a unit to measure the quantity of photons when we model the distribution of the diffracting photons in the following sections.

4.2.2 Deriving Δy

As the 1 mW helium-neon laser used in this experiment emits an uniform output, the distribution of the photons' positions along the *y*-axis in the slit will follow a uniform distribution. Finding the standard deviation of the uniform distribution of the position of photons at each slit width will give the variable of Δy.

For a uniform distribution spanning between the domain $a < x < b$, the standard deviation σ of the distribution is calculated by the formula:

$$\sigma = \sqrt{\frac{(b-a)^2}{12}} \quad [14] \qquad \textit{(Weisstein)}$$

For Δy as the standard deviation of the uniform distribution of *y*, the interval between *b* and *a* is the slit width *d*, hence:

$$\Delta y = \sqrt{\frac{d^2}{12}} \quad [15]$$

All Δy values tabulated on *Table-4* are calculated by using [15].

4.2.3 Deriving Δp_y

To derive Δp_y as the standard deviation of p_y from the collected data, we must first establish a formula that can construct the distribution of diffracting photons as a function of p_y based on the measured *w* and I_0 values. The distribution of diffracting photons as a function of p_y can be modelled after Kirchhoff's diffraction formula:

$$I = I_0 \left[\frac{\sin\left(\frac{\pi d}{\lambda} \sin\theta\right)}{\frac{\pi d}{\lambda} \sin\theta} \right]^2 \quad [16] \quad \textit{(National University of Singapore)}$$

, which predicts the variation of light intensity *I* on any single-slit diffraction pattern as a function of angle θ given the slit width *d*, wavelength λ, and the maximum intensity I_0.

Reviewing *Figure-3* in *Section-1.2* under introduction, it can be deduced that:

$$p_y = p \sin\theta \ [17]$$

, where *p* is the magnitude of the photon's resultant momentum. As the speed of light is constant in the same medium, the magnitude of a photon's resultant momentum must be constant, and it is calculated by rearranging de Broglie's hypothesized formula, [4][4], as follows:

$$p = \frac{h}{\lambda} \ [18]$$

We know that $\lambda = 6.238 \times 10^{-7}$ m for the helium-neon laser used in the experiment, hence substituting this value into [18] gives:

$$p \approx 1.047 \times 10^{-27} \text{ kg m s}^{-1} \ [19]$$

[4] [4]: $\lambda = \frac{h}{p}$ page 9

Substituting [19] into [17], we get:

$$\theta = \arcsin\left(\frac{p_y}{1.047 \times 10^{-27}}\right) \quad [20]$$

Substituting [20] into [16], we get:

$$I = I_0\left[\frac{\sin\left(\frac{\pi d}{\lambda}\left(\frac{p_y}{1.047 \times 10^{-27}}\right)\right)}{\frac{\pi d}{\lambda}\left(\frac{p_y}{1.047 \times 10^{-27}}\right)}\right]^2 \quad [21]$$

, which predicts the variation of light intensity on any single-slit diffraction pattern as a function of p_y given the slit width *d* and the maximum intensity I_0. It should be noted that from this point onward, intensity *I* represents the quantity photons travelling at a particular p_y given [13][5].

As the goal here is to construct the distribution of diffracting photons based on experiment data rather than predicting it, [21] must be further manipulated so that it takes the dependent variable *w* as input instead of the independent variable *d*.

Experiment confirms that the relationship between *d* and *w* is [8][6] at D=1, hence:

$$d = \frac{2\,\lambda}{w} \quad [22]$$

[5] [13]: Photon flux ∝ Light intensity page 21

[6] [8]: $w = \frac{2\,D\,\lambda}{d}$ page 15

Substituting [22] into [21], we finally get:

$$I = I_0 \left[\frac{\sin\left(\frac{2\pi}{w}\left(\frac{p_y}{1.047 \times 10^{-27}}\right)\right)}{\frac{2\pi}{w}\left(\frac{p_y}{1.047 \times 10^{-27}}\right)} \right]^2 \quad [23]$$

, which can be used to construct the distribution of diffracting photons as a function of their momenta in the *y* direction p_y given any pair of *w* and I_0 measurements made from the same diffraction pattern.

A more formal treatment of [23] resolves into the function:

$$\mathrm{I}(p_y) = \begin{cases} I_0, & p_y = 0 \text{ kg m s}^{-1}; \\ I_0 \left[\frac{\sin\left(\frac{2\pi}{w}\left(\frac{p_y}{1.047 \times 10^{-27}}\right)\right)}{\frac{2\pi}{w}\left(\frac{p_y}{1.047 \times 10^{-27}}\right)} \right]^2, & \text{otherwise} \end{cases} \quad [24]$$

$$\{p_y | -1.047 \times 10^{-27} < p_y < 1.047 \times 10^{-27}\}$$

, where $\mathrm{I}(p_y)$ denotes that intensity *I* is treated as a function rather than a variable. The domain of the function is restricted to the stated values because the magnitude of the component momentum p_y cannot be greater than the magnitude of its resultant momentum *p*, which stays constant at $p \approx 1.047 \times 10^{-27}$ kg m s^{-1}.

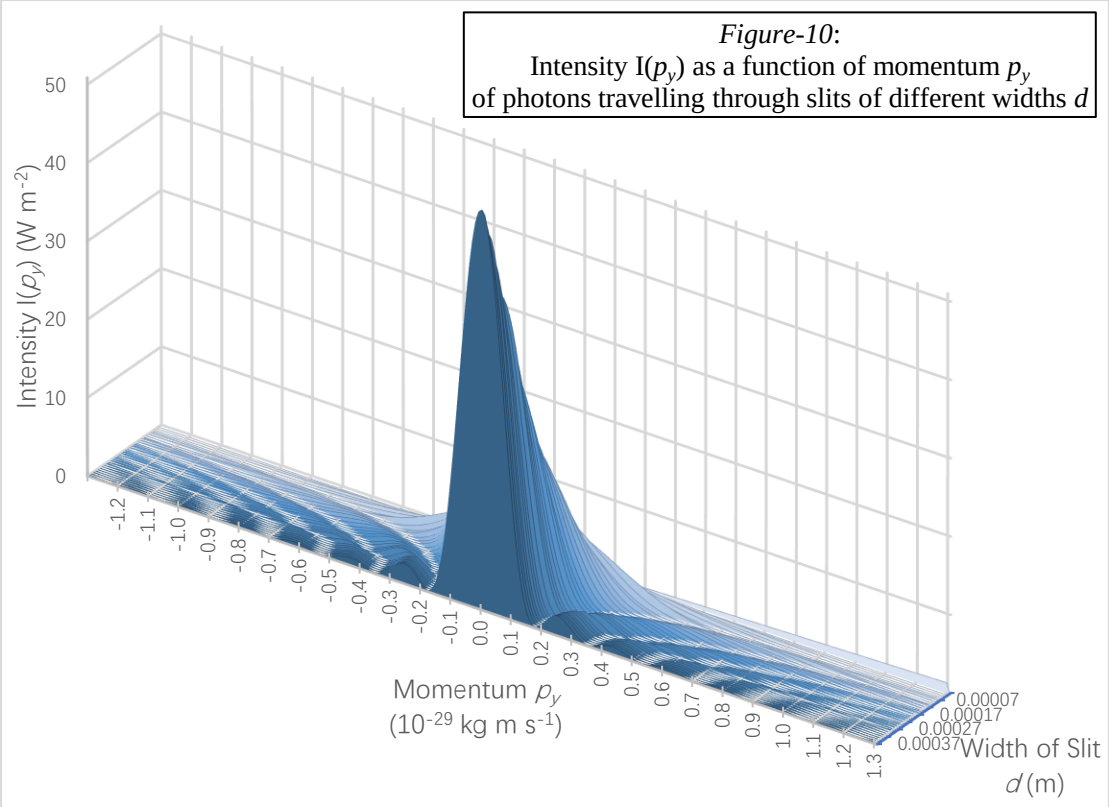

Figure-10:
Intensity I(p_y) as a function of momentum p_y
of photons travelling through slits of different widths d

Inputting each pair of measured average w and I_0 values from *Table-2* and *Table-3* into [24] produces the graph seen on *Figure-10*, which shows the variation of the distribution of diffracting photons as a function of their momentum in the y direction when the slit width changes. Alternatively, *Figure-10* also serves as a better visual representation of how the diffraction pattern becomes more dispersed when the slit narrows.

To calculate Δp_y as the standard deviation of each of the distribution produced at different slit widths on *Figure-10*, we can consider the statistics formula for standard deviation:

$$\sigma = \sqrt{\frac{\sum_{i=1}^{n} f_i(x_i - \mu)^2}{n}} \quad [25]$$

, where x_i stands for each of the value of the data, f_i stands for the statistical frequency that x_i appears, n is the total quantity of data, and μ is the mean of the data set.

If we substitute p_y for x_i, f_i can be substituted by the function $\mathrm{I}(p_y)$ since light intensity can be regarded as a unit measuring the quantity of photons as previously discussed. Taking note that $\mathrm{I}(p_y)$ is a continuous function, the summation expression should be replaced by a definite integral with the domain of $\mathrm{I}(p_y)$, where n as the total quantity of data becomes total area under the function $\mathrm{I}(p_y)$. The following expression is obtained after the aforementioned changes are made to [25]:

$$\sigma = \sqrt{\frac{\int_{-1.047\times10^{-27}}^{1.047\times10^{-27}} I(p_y) \times (p_y - \mu)^2 \, dp_y}{\int_{-1.047\times10^{-27}}^{1.047\times10^{-27}} I(p_y) \, dp_y}} \quad [26]$$

$\mathrm{I}(p_y)$ as of [24] is an even function, hence $\mu = 0$; Therefore the finalized equation for calculating Δp_y is:

$$\Delta p_y = \sqrt{\frac{\int_{-1.047\times10^{-27}}^{1.047\times10^{-27}} I(p_y) \times {p_y}^2 \, dp_y}{\int_{-1.047\times10^{-27}}^{1.047\times10^{-27}} I(p_y) \, dp_y}} \quad [27]$$

All Δp_y values tabulated on *Table-4* are calculated by using [27].

4.3 Relationship between Δp_y and Δy of diffracting photons

Table-4: Relationship between uncertainty of position and uncertainty of momentum of diffracting photons

Independent Variables		Dependent Variables		
d: Width of slit (m) *± 0.000005 m instrument error*	Δy: Uncertainty of position of photons (m) *± 1.44E-06 m*	*w*: Average width of principle maxima (m) *with aggregate error*	I_0: Average maximum intensity (W m^{-2}) *with propagated error*	Δp_y: Uncertainty of momentum in the *y* direction (kg m s^{-1}) *with propagated error*
0.000370	0.000107	0.0034 ± 0.0001	51.0 ± 0.1	6.3E-30 ± 2E-31
0.000360	0.000104	0.0034 ± 0.0001	49.6 ± 0.4	6.1E-30 ± 2E-31
0.000350	0.000101	0.0034 ± 0.0001	48 ± 1	6.1E-30 ± 3E-31
0.000340	0.000098	0.0035 ± 0.0001	47 ± 1	6.5E-30 ± 3E-31
0.000330	0.000095	0.0035 ± 0.0001	45.2 ± 0.8	6.5E-30 ± 3E-31
0.000320	0.000092	0.0035 ± 0.0001	44.0 ± 0.7	6.5E-30 ± 3E-31
0.000310	0.000089	0.0036 ± 0.0001	42.2 ± 0.7	6.6E-30 ± 3E-31
0.000300	0.000087	0.0036 ± 0.0003	39.9 ± 0.6	7.0E-30 ± 6E-31
0.000290	0.000084	0.0039 ± 0.0003	39.0 ± 0.5	7.6E-30 ± 6E-31
0.000280	0.000081	0.0043 ± 0.0002	38.4 ± 0.3	8.8E-30 ± 5E-31
0.000270	0.000078	0.0043 ± 0.0002	35.5 ± 1.9	8.8E-30 ± 8E-31
0.000260	0.000075	0.0044 ± 0.0002	33.9 ± 0.9	9.0E-30 ± 7E-31
0.000250	0.000072	0.0046 ± 0.0001	30.6 ± 0.8	9.1E-30 ± 4E-31
0.000240	0.000069	0.0047 ± 0.0003	29.3 ± 0.8	9.6E-30 ± 8E-31
0.000230	0.000066	0.0051 ± 0.0003	28.1 ± 0.6	1.05E-29 ± 8E-31
0.000220	0.000064	0.0053 ± 0.0004	26.4 ± 0.7	1.1E-29 ± 1E-30
0.000210	0.000061	0.0055 ± 0.0005	23.3 ± 0.7	1.2E-29 ± 2E-30
0.000200	0.000058	0.0057 ± 0.0005	23 ± 2	1.2E-29 ± 2E-30
0.000190	0.000055	0.0061 ± 0.0005	21 ± 1	1.3E-29 ± 2E-30
0.000180	0.000052	0.0066 ± 0.0007	20 ± 1	1.4E-29 ± 2E-30
0.000170	0.000049	0.0070 ± 0.0008	18.5 ± 0.3	1.5E-29 ± 2E-30
0.000160	0.000046	0.0073 ± 0.0009	17 ± 1	1.5E-29 ± 3E-30
0.000150	0.000043	0.008 ± 0.001	15 ± 1	1.7E-29 ± 4E-30
0.000140	0.000040	0.0087 ± 0.0006	12 ± 1	1.8E-29 ± 2E-30
0.000130	0.000038	0.0090 ± 0.0009	10 ± 1	1.9E-29 ± 4E-30
0.000120	0.000035	0.010 ± 0.002	9.8 ± 0.8	2.1E-29 ± 5E-30
0.000110	0.000032	0.012 ± 0.002	8 ± 1	2.5E-29 ± 8E-30
0.000100	0.000029	0.012 ± 0.002	5.8 ± 0.9	2.4E-29 ± 7E-30
0.000090	0.000026	0.014 ± 0.002	3.6 ± 0.2	2.8E-29 ± 6E-30
0.000080	0.000023	0.017 ± 0.005	2.6 ± 0.3	3E-29 ± 1E-29
0.000070	0.000020	0.019 ± 0.003	1.7 ± 0.1	3.2E-29 ± 7E-30
0.000060	0.000017	0.023 ± 0.001	1.1 ± 0.1	4.0E-29 ± 5E-30
0.000050	0.000014	0.028 ± 0.005	0.32 ± 0.02	5E-29 ± 1E-29

Figure-11: Relationship between uncertainty of position Δy and uncertainty of momentum Δp_y

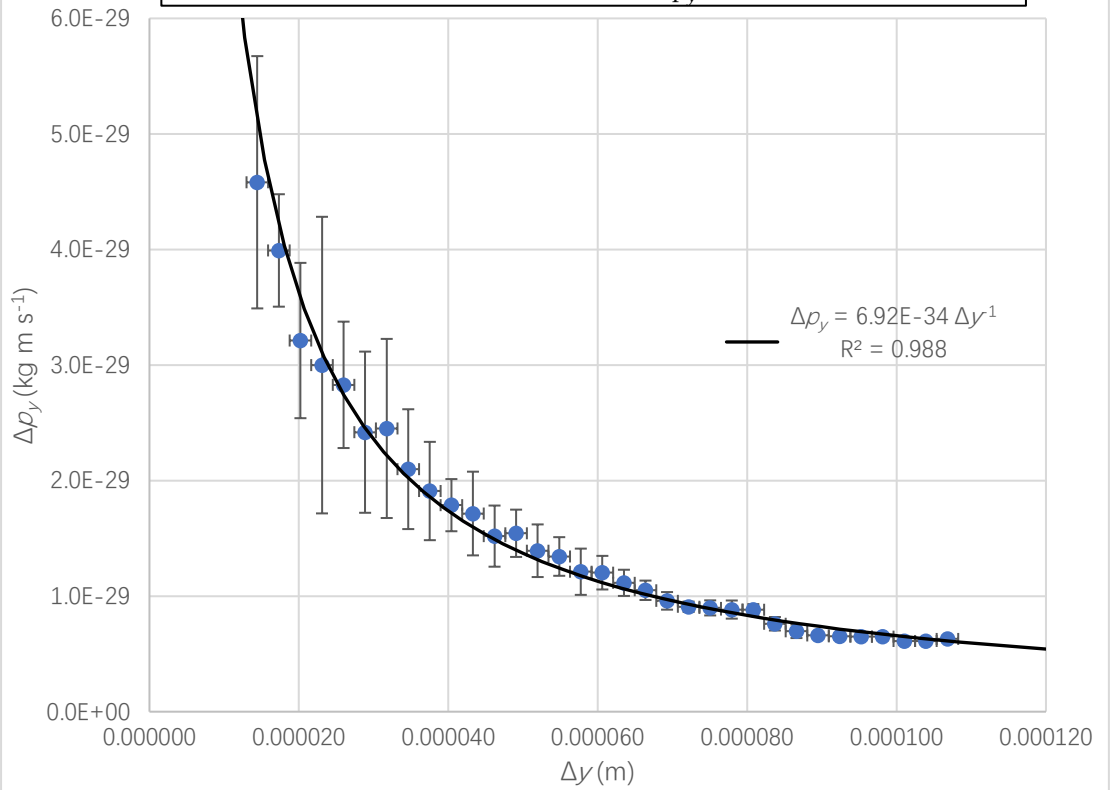

Figure-12: Linearized relationship between Δy and Δp_y

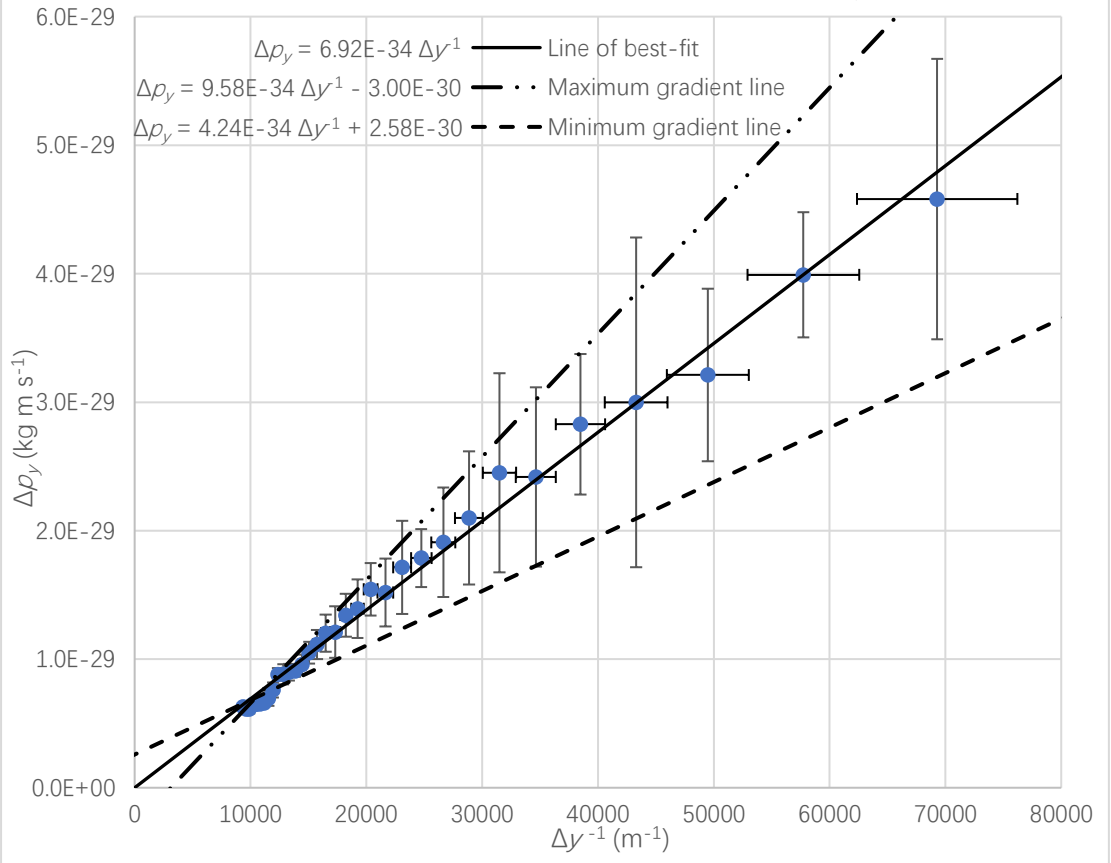

While *Figure-11* shows the relationship between Δy and Δp_y, the gradient of the linear trend lines on *Figure-12* represents the value of the constant *k* in the anticipated relationship [2][7], where *k* is the fundamental limit of the products of Δy and Δp_y of the diffracting photons.

The line of best-fit on *Figure-12* and *Figure-11* both have the equation:

$$\Delta p_y = 6.92 \times 10^{-34}\, \Delta y^{-1} \quad [28]$$

, showing that the best-fit value of *k* for the dataset on *Table-4* is:

$$k = 6.92 \times 10^{-34}\ \mathrm{m^2\ kg\ s^{-1}}.$$

The margin of error for the possible range of *k* values that can be derived from *Figure-12* is determined by using the following formula:

$$k = m \pm \frac{m_{max} - m_{min}}{2}$$

, given:

Best-fit gradient $m = 6.92 \times 10^{-34}\ \mathrm{m^2\ kg\ s^{-1}}$
Maximum gradient $m_{max} = 9.58 \times 10^{-34}\ \mathrm{m^2\ kg\ s^{-1}}$
Minimum gradient $m_{min} = 4.24 \times 10^{-34}\ \mathrm{m^2\ kg\ s^{-1}}$

, which after rounding to one significant figure of error gives:

$$k = (7 \pm 3) \times 10^{-34}\ \mathrm{m^2\ kg\ s^{-1}} \quad [29]$$

Hence, the experiment ultimately shows that

$$\Delta y\, \Delta p_y = (7 \pm 3) \times 10^{-34}\ \mathrm{m^2\ kg\ s^{-1}} \quad [30]$$

for photons diffracting through narrow slits of varying widths.

[7] [2]: $\Delta y\, \Delta p_y = k,\ \ k \in \mathbb{R}^+$ page 8

5. Conclusion

There is substantial evidence to support that the single slit diffraction of monochromatic coherent light does demonstrate Heisenberg's uncertainty principle.

Firstly, [28] as the best-fit model on both *Figure-11* and *Figure-12* clearly shows an inversely proportional relationship between Δy and Δp_y, which strongly agrees with [2] as the hypothesized relationship. [28] deviates from each data point plotted on both *Figure-11* and *Figure-12* within the acceptable margin of error, while its coefficient of determination with the data points plotted on *Figure-11* is $R^2 = 0.988$, which shows that it is both a valid and a relatively accurate model of the dataset from *Table-4*

Secondly, the experimental value of k derived from *Figure-12* as the fundamental limit of the products of Δy and Δp_y for diffracting photons strongly agrees with [5][8] as the literature relationship for diffracting electrons, which states that Planck's constant h is the fundamental limit of the product between Δy and Δp_y. Noting that $\mathrm{J\,s}$ is equivalent to $\mathrm{m^2\ kg\ s^{-1}}$, the literature value of $k = h \approx 6.63 \times 10^{-34}\ \mathrm{J\,s}$ in [5] falls well within the margin of error given by [29], while the best-fit value of $k = 6.92 \times 10^{-34}\ \mathrm{m^2\ kg\,s^{-1}}$ derived from [28] only deviates from Planck's constant by approximately 4.2%.

Therefore, it can be solidly concluded that the relationship between the width of a single slit and the dispersion of the diffraction pattern formed when monochromatic coherent light passes through it does demonstrate Heisenberg's uncertainty principle.

[8] [5]: $\Delta y\, \Delta p_y \cong h$ page 9

6. Evaluation

6.1 Limitations of experiment setup

A significant limitation of the experiment setup lies with using a micrometer to adjust the slit width. The micrometer used in the experiment changes the slit width through two metal rods, where one rod moves towards another when the slit width is restricted. As seen from *Figure-13*, this limitation makes it impossible for the slit to remain at the exact center of the laser dot, which causes the diffraction produced by the setup to be slightly asymmetrical in terms of light intensity as seen on *Figure-14.*

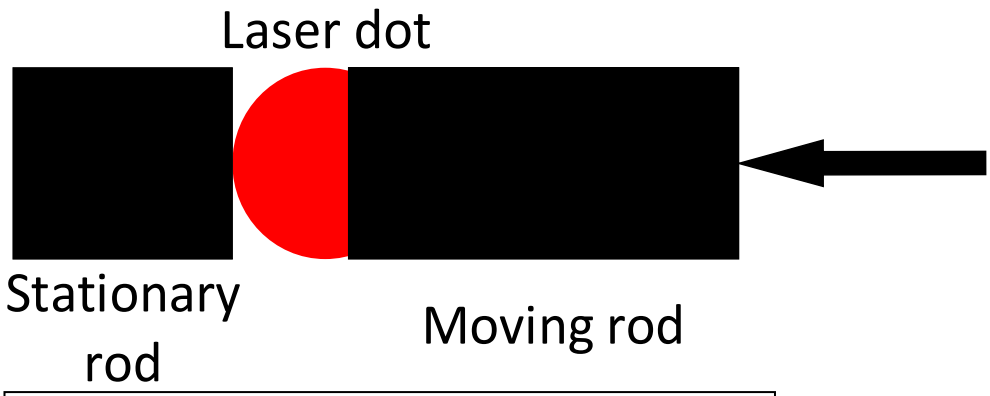

Figure-13: The mechanism of using a micrometer to control slit width

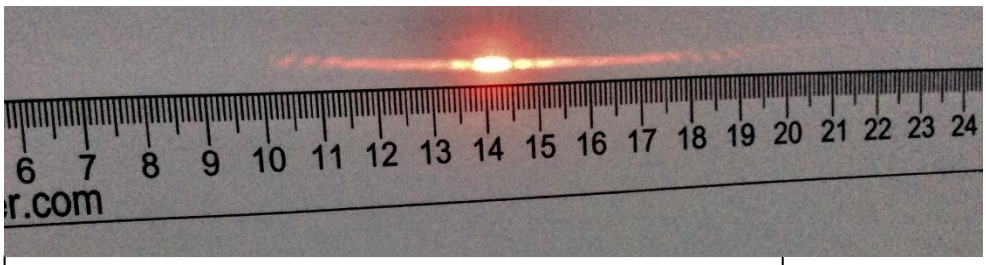

Figure-14: Photo of one of the diffraction pattern produced during the experiment, the right side is slightly brighter than the left side

With reference to *Figure-9*, this limitation is potentially what caused the rate of change of I_0 to decrease at narrower slit widths, where the slit becomes more and more off-

center in terms of its position with the laser dot. If this were the case, there would be a systematic error for the measurement of I_0 in the experiment.

However, this limitation did not have a significant adverse effect on the reliability of the results of the experiment. Firstly, the affected variable I_0 can be cancelled out during the calculation for Δp_y by isolating it as a constant from the integral expressions involving the function $\mathrm{I}(p_y)$, which means that the proximate systematic error will not be carried forward to the ultimate dependent variable of Δp_y. Secondly, *Figure-7* shows that the measured widths of the central maxima largely agrees with the literature values within the acceptable margin of error, which means that the overall geometry of the diffraction patterns remained relatively intact despite the flaw in the experiment setup.

This limitation can be readily resolved if more professional equipment, such as the Vernier diffraction apparatus (*Vernier software & technology)*, were available. The slit of the Vernier diffraction apparatus will always be positioned at the exact center of the light source, and hence will always produce a symmetrical diffraction pattern.

6.3 Scope of further research

One question remain unanswered by this investigation is whether photons exhibit the classical uncertainty inequality $\Delta x\, \Delta p \geq \frac{h}{4\pi}$ on a three-dimensional scale. Although it is not experimentally feasible to evaluate the three-dimensional uncertainty principle of diffracting photons, a meaningful extension to this investigation would be to experimentally derive the two-dimensional uncertainty principle of diffracting

photons by passing laser through a circular aperture instead of a slit. This way we can further confirm that the diffraction of light is caused by photons obeying Heisenberg's uncertainty principle in two dimensions, and potentially extrapolate on the three-dimensional uncertainty relation based on the results obtained for the uncertainty relations in one and two dimensions.

3989 words

excluding figures, tables, equations and annotations.

Works cited

Belle, Jean Louis Van. Diffraction and the Uncertainty Principle (I). *Reading Feynman*, 21 Sept. 2014, readingfeynman.org/2014/09/20/diffraction-and-the-uncertainty-principle/. Accessed 3 Aug. 2018.

Georgia State University. Luminous Efficacy Tables. *Hyper Physics*, Georgia State University, hyperphysics.phy-astr.gsu.edu/hbase/vision/efficacy.html. Accessed 1 July. 2018.

Georgia State University. Single Slit Diffraction. *Hyper Physics*, Georgia State University, hyperphysics.phy-astr.gsu.edu/hbase/phyopt/sinvar.html. Accessed 17 May. 2018.

Heisenberg, Werner, et al. *The Physical Principles of the Quantum Theory*. Dover Publ., 2009, p.14.

National University of Singapore. Physics for Electrical Engineers - Single Slit Diffraction. *NUS Physics*, National University of Singapore, www.physics.nus.edu.sg/~ephysics/documents/PC2232-Diffraction-revised.pdf. Accessed 25 May. 2018.

University of Colorado Boulder. *Topic 14. Wavefronts and Huygen's Principle*. University of Colorado Boulder, www.colorado.edu/physics/phys1230/phys1230_fa01/topic14.html. Accessed 25 May. 2018.

University of New Mexico. Uncertainty in Free Particle Waves. Physics Course Notes, University of New Mexico, physics.unm.edu/Courses/Fields/Phys491/Notes/UncertaintyinFreeParticleWaves.pdf. Accessed 5 Aug. 2018.

University of Sydney. *Heisenberg Uncertainty Principle*. University of Sydney, www.physics.usyd.edu.au/teach_res/hsp/eq/eq25.pdf. Accessed 25 May. 2018.

Vernier Software & Technology. Diffraction Apparatus. *Products*, Vernier Software & Technology, www.vernier.com/products/sensors/dak/. Accessed 10 Aug. 2018.

Weisstein, Eric. Uniform Distribution. *Wolfram MathWorld*, 2002, mathworld.wolfram.com/UniformDistribution.html. Accessed 28 July. 2018.

Appendix

Table including different conversion factors between luminous intensity and light intensity at varying wavelengths *(Georgia State University, Luminous Efficacy Tables)*

Wavelength λ (nm)	Photopic Luminous Efficacy V_λ	Photopic Conversion lm/W	Scotopic Luminous Efficacy V'_λ	Scotopic Conversion lm/W
380	0.000039	0.027	0.000589	1.001
390	0.000120	0.082	0.002209	3.755
390	0.000120	0.082	0.002209	3.755
400	0.000396	0.270	0.009290	15.793
410	0.001210	0.826	0.034840	59.228
420	0.004000	2.732	0.096600	164.220
430	0.011600	7.923	0.199800	339.660
440	0.023000	15.709	0.328100	557.770
450	0.038000	25.954	0.455000	773.500
460	0.060000	40.980	0.567000	963.900
470	0.090980	62.139	0.676000	1149.200
480	0.139020	94.951	0.793000	1348.100
490	0.208020	142.078	0.904000	1536.800
500	0.323000	220.609	0.982000	1669.400
507	0.444310	303.464	1.000000	1700.000
510	0.503000	343.549	0.997000	1694.900
520	0.710000	484.930	0.935000	1589.500
530	0.862000	588.746	0.811000	1378.700
540	0.954000	651.582	0.655000	1105.000
550	0.994950	679.551	0.481000	817.700
555	1.000000	683.000	0.402000	683.000
560	0.995000	679.585	0.328800	558.960
570	0.952000	650.216	0.207600	352.920
580	0.870000	594.210	0.121200	206.040
590	0.757000	517.031	0.065500	111.350
600	0.631000	430.973	0.033150	56.355
610	0.503000	343.549	0.015930	27.081
620	0.381000	260.223	0.007370	12.529

630	0.265000	180.995	0.003335	5.670
640	0.175000	119.525	0.001497	2.545
650	0.107000	73.081	0.000677	1.151
660	0.061000	41.663	0.000313	0.532
670	0.032000	21.856	0.000148	0.252
680	0.017000	11.611	0.000072	0.122
690	0.008210	5.607	0.000035	0.060
700	0.004102	2.802	0.000018	0.030
710	0.002091	1.428	0.000009	0.016
720	0.001047	0.715	0.000005	0.008
730	0.000520	0.355	0.000003	0.004
740	0.000249	0.170	0.000001	0.002
750	0.000120	0.082	0.000001	0.001
760	0.000060	0.041	0.000000	0.000
770	0.000030	0.020	0.000000	0.000